

High Spatial Resolution Microwave Detection System for Brillouin-based Distributed Temperature and Strain Sensors

Mohamed N. Alahbabi[†], Nicholas P. Lawrence, Yuh T. Cho and Trevor P. Newson

[†] Optoelectronics Research Centre, University of Southampton, Southampton, SO17 1BJ, UK

E-mail: mna@orc.soton.ac.uk

Abstract. We present a microwave detection system for coherent detection of spontaneous Brillouin-based distributed temperature and strain measurements. The system was designed to overcome the existing bandwidth limitations of a previously used commercial spectrum analyzer and provide a commercially practical solution to the detection of the Brillouin frequency shift and intensity for long range high spatial resolution measurements. The detection system bandwidth corresponds to a potential spatial resolution of ~ 60 cm. The system was demonstrated as temperature sensor over a range of 30km, with a temperature resolution of 1.6°C , spatial resolution of ~ 2 m. It was also demonstrated as a combined temperature and strain sensor over a range of 6.3km with ~ 1.3 m spatial resolution, temperature and strain resolution of 3°C and $80\mu\epsilon$ respectively were achieved.

Submitted to: *Meas. Sci. Technol.*

Key Words: *Optical Fiber Sensors, Brillouin Scattering, Distributed Temperature and Strain Measurements.*

1. Introduction

Distributed optical fibre sensors based on Brillouin scattering with sub-meter spatial resolution capabilities have been previously reported, but were confined to relatively short sensing lengths and focused on either measuring the Brillouin frequency shift [1] or intensity [2]. Several applications such as the continuous monitoring of temperature/strain in underground power cables, live optical links and large scale structures require sensors with relatively high spatial resolution combined with long range [3, 4]. It is now well established that the Brillouin frequency shift and the change in its intensity may be used to obtain simultaneously temperature and strain change along a link of fibre [5, 6].

Coherent detection of the anti-Stokes Brillouin signal has proved to be a particularly promising approach, but the long range sensor previously described [7], required electrical detection in the microwave realm, as the detected Brillouin backscatter beat signal lies between 10.5-11.5GHz. Modern photo-detectors and electronic spectrum analyzers (ESAs) can readily process such signals but the majority of ESAs are designed to maximize the frequency resolution capability i.e. have narrow resolution bandwidth, operate at relatively low-intermediate frequencies (IF) and have correspondingly low video bandwidths leading to poor spatial resolution.

In our previous reported work, using such an ESA, the spatial resolution was limited to 20m [7, 8]. Our present application for monitoring temperature in power cables required a spatial resolution up to 1m. Other potential applications of our system are to monitor strain with similar spatial resolution in large scale structures i.e. dams, bridges, tunnels and buildings. To achieve such spatial resolution, requires an ESA with a higher video bandwidth and a broader resolution bandwidth than was available at an economic price. In this paper we present a microwave detection system designed to achieve this order

of magnitude improvement in spatial resolution. The system was tested as a long range distributed temperature sensor with $\sim 2\text{m}$ spatial resolution over 30km, and as a simultaneous temperature and strain measurement system with $\sim 1.3\text{m}$ spatial resolution over 6.3km.

2. Principle of Operation

The principle of Brillouin Optical Time-Domain Reflectometry (BOTDR) with optical coherent detection was employed, see figure 1. A single laser was used both as a source for generating the probe pulse and as an optical local oscillator (OLO) for coherent detection of the backscattered anti-Stokes Brillouin signal. The generated beat signal was around 11GHz, corresponding to the Brillouin frequency shift. This was mixed with a PC controlled YIG-based electrical local oscillator (ELO) and passed through a band-pass filter (BPF) centred at 1GHz, bandwidth 50MHz to generate an IF of 1GHz. The ELO was scanned through a range of frequencies in user-defined frequency steps. The selected frequency of the ELO determined the Brillouin beat frequency that was measured: i.e. the measured component of the Brillouin spectrum was equal to the ELO frequency plus the 1GHz IF, less 110MHz due to the frequency shift induced by the acousto-optic modulator (AOM) generating the pulse. The BPF characteristics are shown in figure 2. The down-converted IF signal was amplified and then rectified using a microwave diode rectifier generating a signal proportional to the intensity of the Brillouin backscatter at the chosen frequency. The rectified signal was fed to a storage oscilloscope, which was used to average a large number of time domain traces that were then transferred to the PC. The Brillouin spectra were built by collecting such traces over a range of frequencies determined by the YIG synthesizer. The Brillouin frequency spectrum and Brillouin intensity change were then extracted from the collected data

and hence, allowing the temperature/strain change to be spatially resolved.

3. System Set-up and Measurements

The experimental arrangement for the coherent detection of the anti-Stokes spontaneous Brillouin backscatter using the microwave detection system is shown in figure 1. The source was a tuneable laser @ 1533.2nm, with ~ 1 MHz line width, and $100\mu\text{W}$ CW output. In the initial long range experiment, two Erbium doped fibre amplifiers (EDFAs) and an acousto-optic modulator were used to generate a probe pulse of 25mW, 20ns with repetition rate of 84Hz which was launched into the 32km sensing fibre. An EDFA preamplifier was used to amplify the weak backscattered signal generated in the sensing fibre prior to mixing with a 1.8mW OLO. The Bragg grating (reflectivity = 99.4%, $\Delta\lambda_g = 0.12\text{nm}$, $\lambda_g = 1533.11\text{nm}$) was centred at the Brillouin frequency. This arrangement allowed transmission of the local optical oscillator, whilst filtering the Brillouin anti-Stokes signal from the Rayleigh signal. A 20GHz lightwave detector and the microwave detection system allowed the collection of time domain traces centred at the desired RF frequencies. The sensing fibre was standard single mode fibre (SMF) in 3 sections, fusion spliced and arranged as shown in figure 1. The first 30km remained on the original spools at room temperature. The next 400m were placed in an oven at 60°C . The subsequent 1.6km was maintained at room temperature and zero strain as a reference.

To determine the spatial resolution and accuracy of the system, Brillouin frequency measurements were taken between 30 and 30.8km where the central 400m length of fibre was heated to 60°C , and the remaining fibre was at room temperature of 20°C . The temperature change along the sensing fibre was determined by analyzing the frequency shift of the Brillouin backscatter. Brillouin spectra were built from 15 separate backscatter traces, each averaged 2^{15} times, taken every 10MHz, starting at 10.99GHz.

A Lorentzian curve was fitted to each spectrum and the peak frequency was evaluated at each point along the sensing fibre.

To further demonstrate the capability of the microwave detection system with regard to spatial resolution, a second experiment was performed in which the AOM was replaced with an electro-optic modulator (EOM) which allowed the pulse width to be reduced from 20ns to 10ns. The temperature and strain were measured simultaneously over a range of 6.3km. In this experiment, a 7m of fibre was loosely coiled and placed in an oven at 80 °C to allow heating whilst ensuring zero strain. Another 7m was passed around two pairs of pulleys and loaded with weights suspended at the end of the rig, such that the fibre was stretched by 11.2mm which corresponds to a strain of $\sim 1600\mu\epsilon$ [7]. A length of 25m was inserted between the two sections at room temperature and zero strain as a reference. Both the Brillouin frequency shift and its intensity were measured simultaneously using the microwave detection system. Brillouin intensity was measured by evaluating the sum of Brillouin spectrum components at each point along the sensing fibre and was normalized by the Rayleigh trace to account for the fibre loss [5]. All Brillouin frequency shift measurements were referenced to room temperature and zero strain. These two normalized traces were used to derive temperature and strain variations along the sensing fibre. To enable such measurements, previously measured values of the temperature and strain dependence of Brillouin frequency shift and its backscattered intensity accompanied with the two equations which relate temperature and strain to Brillouin frequency shift and its intensity were used [7]. The two variables of strain and temperature were determined using the following equations:

$$\Delta T = \frac{K_\epsilon^\nu \Delta P - K_\epsilon^P \Delta \nu}{K_\epsilon^\nu K_T^P - K_\epsilon^P K_T^\nu} \quad (1)$$

$$\Delta \epsilon = \frac{K_T^P \Delta \nu - K_T^\nu \Delta P}{K_\epsilon^\nu K_T^P - K_\epsilon^P K_T^\nu} \quad (2)$$

Where $\Delta\nu$ and ΔP are the frequency shift and intensity change, K_T^ν and K_ε^ν are temperature and strain coefficients governing frequency shifts with 1.07MHz/°C and 0.048MHz/ $\mu\varepsilon$ respectively, and K_T^P and K_ε^P are the coefficients for power variations with respect to temperature 0.36%/°C and strain $-9 \times 10^{-4}\%$ / $\mu\varepsilon$ respectively [7]. The corresponding errors in the derived temperature and strain measurements are given by [7].

$$\delta T = \frac{|K_\varepsilon^P \delta\nu| + |K_\varepsilon^\nu \delta P|}{|K_\varepsilon^\nu K_T^P - K_\varepsilon^P K_T^\nu|} \quad (3)$$

$$\delta\varepsilon = \frac{|K_T^P \delta\nu| + |K_T^\nu \delta P|}{|K_\varepsilon^\nu K_T^P - K_\varepsilon^P K_T^\nu|} \quad (4)$$

Where $\delta\nu$ and δP are the measured RMS error on the Brillouin frequency and intensity respectively.

4. Results and Discussion

Figure 3 shows the temperature change at the heated section derived from the shift in Brillouin frequency. A temperature sensitivity of 1.07 ± 0.07 MHz/°C was measured. This is in agreement with previously reported results [7, 9]. The spatial resolution in the first experiment was limited by the rise time of the available modulator AOM used to generate the probe pulse, which limit the pulse width to ~ 20 ns. For clarity, figure 4 shows a 10-90% rise-time that was measured at the front end of the sensing fibre and agrees with the expected performance governed by the duration of the pulse and not by the electronics of the detection system. The power trace was found to be too noisy to allow useful simultaneous measurements at this distance. The sensor was able to record temperature changes of less than 1.1 °C up to 20km. The error increased with distance, but was less than 1.7 °C at the end of the sensing length, see figure 5.

In the second experiment, the microwave detection system was demonstrated for combined strain and temperature measurements and used an EOM to reduce the pulse

width to $\sim 10\text{ns}$ to achieve higher spatial resolution. The derived temperature and strain changes along the sensing fibre were obtained using (1) and (2) and are shown in figure 6. The corresponding temperature and strain resolution were calculated using (3) and (4) based on the frequency and intensity errors at the heated and strain sections. For frequency error of 0.7MHz and 1.2% intensity error, temperature resolution of about 3°C and the strain resolution of $\sim 80\mu\epsilon$ respectively were calculated. The variation in strain over the strained region is attributed to the friction in the pulley system. The spatial resolution verification measurement was made at 600m down the sensing fibre and was defined by the (10-90%) response time with a sampling resolution of 20cm . It was found to be $\sim 1.3\text{m}$, see inset plot in figure 6(a). The accuracy of the simultaneous measurements was investigated up to 10km of sensing range using the same conditions as in the simultaneous measurement. The frequency and intensity resolutions were evaluated at 2km intervals averaged over a length of 100m , see figure 7. These values were used to derive the temperature and strain resolutions, and shown in figure 8. It was found that the noise on the intensity trace is responsible for more than 90% of the temperature and strain errors, indicating that the intensity measurements are the limiting factor on the accuracy of the simultaneous temperature and strain measurements. The system's accuracy may be improved by performing more time domain traces averages which will reduce noise but increase the measurement time. The rise time of the currently used RF diode rectifier $\sim 10\text{ns}$ presently places an upper limit on the system's spatial resolution, but we believe our detection system is now potentially capable of $\sim 60\text{cm}$ spatial resolution provided its BPF bandwidth is tuned to its maximum ($\sim 80\text{MHz}$), and a faster microwave diode rectifier is used.

5. Conclusion

In conclusion, a microwave detection system has been designed and tested for coherent detection of the backscattered spontaneous anti-Stokes Brillouin signals for distributed temperature/strain sensors. The aim was to improve the spatial resolution of our previously reported results by an order of magnitude and this has been achieved. The RMS temperature error in the long range experiment was 1.6°C over a 30km range with a spatial resolution of $\sim 2\text{m}$. Simultaneous measurement of temperature and strain then demonstrated using a faster modulator; 3°C temperature resolution and $80\mu\epsilon$ strain resolution were achieved with $\sim 1.3\text{m}$ spatial resolution over 6.3km of sensing range. The design represents an important and necessary advance for constructing a commercial sensor as it dispenses with the previous need for an expensive ESA. It also promises practical high spatial resolution and accurate long range Brillouin-based distributed optical sensing systems, with potential for further improvements in spatial resolution.

References

- [1] Hotate K and Hasegawa T 2000, Measurement of Brillouin gain spectrum distribution along an optical fibre using a correlation-based technique-proposal, experiment and simulation. *IEICE Trans. Electron.* **E83** p 405-411.
- [2] Kee H, Lees G and Newson T P 2000, 1.5m Brillouin-based fibre optic distributed temperature sensor with high spatial resolution of 20cm. *OFS 2000 Venice 11-13* p 3-30.
- [3] Wait P and Hartog A 2001, Spontaneous Brillouin-based distributed temperature sensor utilizing a fiber Bragg grating notch filter for the separation of the Brillouin signal. *IEEE Photonics Technology Letters* **13** p 508-510.
- [4] Wild F de , Schmetz P 2000, The application of optical sensors for temperature, mechanical stress and moisture in energy cables in the Netherlands. *OFS Digest 1* p 820-823.
- [5] Wait P and Newson T P 1996, Landau-Placzek ratio applied to distributed fiber sensing. *Optics Communications* **122** p 141-146.
- [6] Parker T and *et al.* 1997, A Fully distributed simultaneous strain and temperature sensor using spontaneous Brillouin backscatter. *IEEE Photonics Technology Letters* **9** p 979-981.
- [7] Maughan S, Kee H and Newson T P 2001, Simultaneous distributed fibre temperature and strain sensor using microwave coherent detection of spontaneous Brillouin backscatter *Measurements Science and Technology* **12** p 834-842.
- [8] Hewlett Packard 1999, Spectrum Analyzers: Optimizing spectrum analyzer amplitude accuracy. *Hewlett Packard* **E** p 5963.
- [9] Parker T and *et al.* 1997, Temperature and strain dependence of the power level and frequency of spontaneous Brillouin scattering in optical fibers. *Optics Letters* **22** p 787-789.

List of Figures

- (i) **Figure-1** Experimental arrangement for measuring Brillouin frequency shift using microwave detection system. EDFA=erbium-doped fibre amplifier, AOM=acousto-optic modulator, PS=polarization scrambler, LO=local oscillator, BG=bragg grating, C=circulator, LD=lightwave detector, YIG= YIG synthesizer, BPF= band pass filter.
- (ii) **Figure-2** Transmission window of the 1GHz BPF and the down converted Brillouin spectrum.
- (iii) **Figure-3** Temperature change at the heated section in the long range experiment.
- (iv) **Figure-4** A (10-90%) rise-time of temperature change at 600m down the sensing fibre indicating spatial resolution of ~ 2 m.
- (v) **Figure-5** The RMS temperature errors for the 20ns pulse width measurements along the sensing fibre at 5km intervals average over a length of 500m.
- (vi) **Figure-6** (a) The derived temperature and (b) the derived strain for the simultaneous temperature and strain measurements respectively. The inset graph in (a) verified the 1.3m spatial resolution measured at 600m down the sensing fibre, which is defined by 10-90% percentage response.
- (vii) **Figure-7** (a) Frequency resolution, (b) intensity resolution taken over 100m window at 2km intervals. The error bars indicate ± 1 Standard Deviation.
- (viii) **Figure-8** Derived resolutions of temperature (left) and strain (right) based upon the measured data in figure 7.

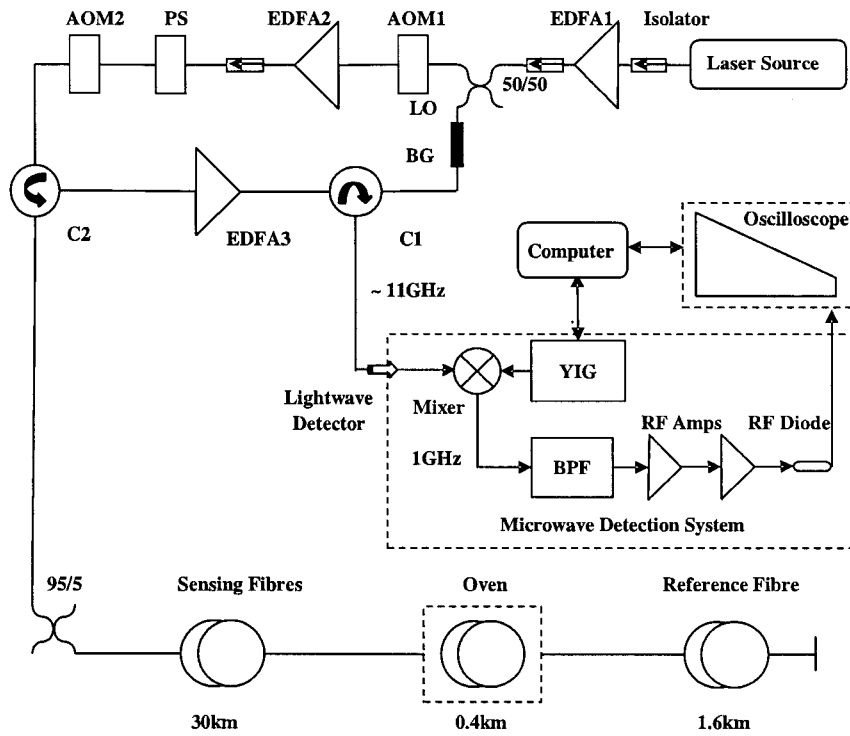


Figure 1. Experimental arrangement for measuring Brillouin frequency shift using microwave detection system. EDFA=erbium-doped fibre amplifier, AOM=acousto-optic modulator, PS=polarization scrambler, LO=local oscillator, BG=bragg grating, C=circulator, LD=lightwave detector, YIG= YIG synthesizer, BPF= band pass filter..

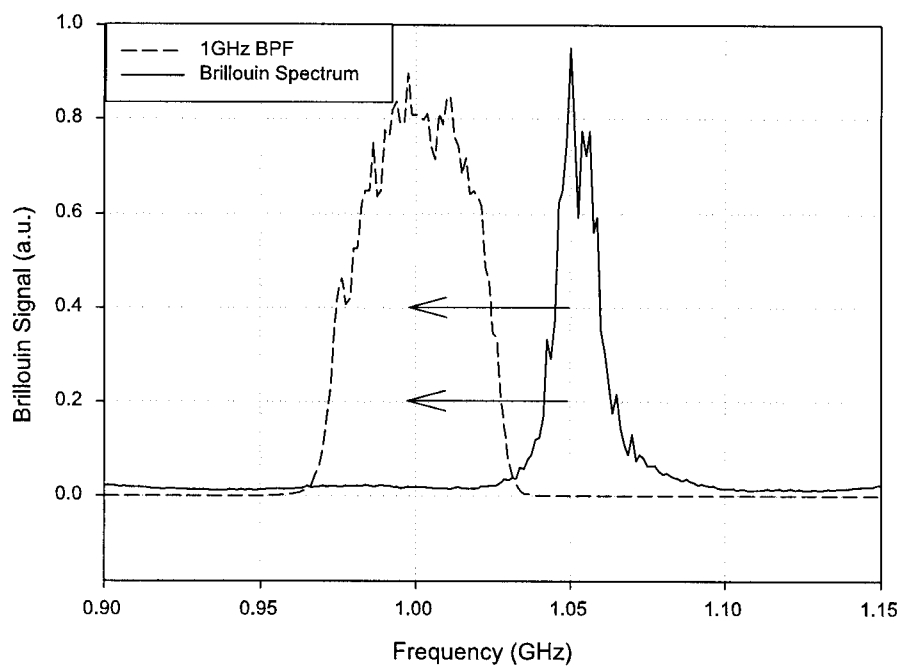


Figure 2. Transmission window ($\sim 50\text{MHz}$) of the 1GHz BPF and the down converted Brillouin spectrum.

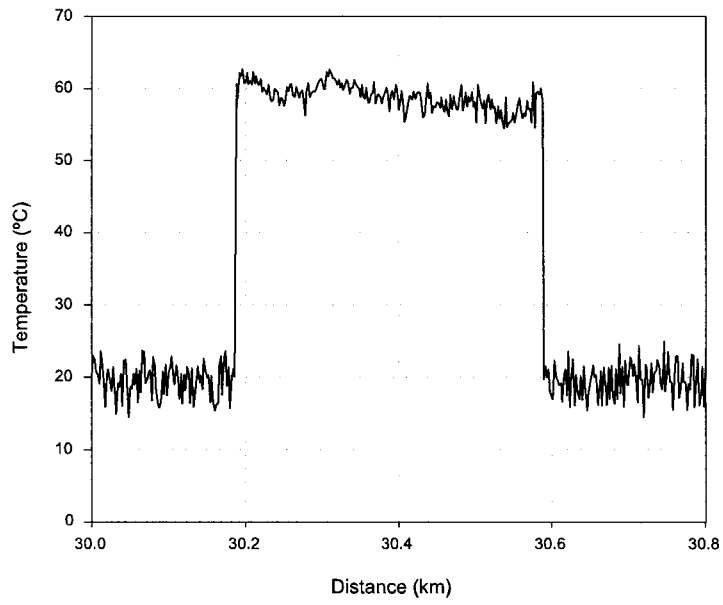


Figure 3. Temperature change at the heated section in the long range experiment.

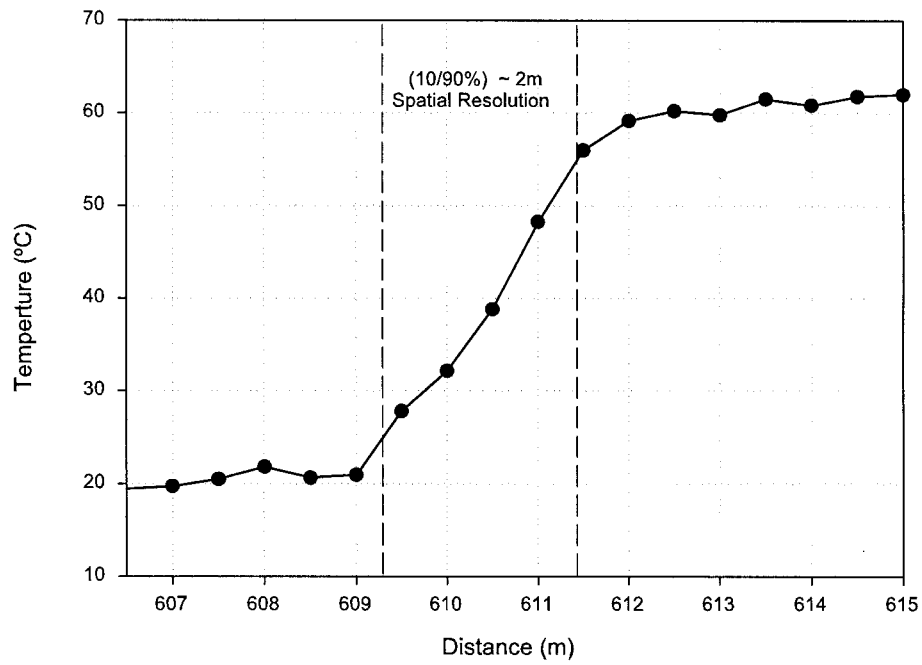


Figure 4. A (10-90%) rise-time of temperature change at 600m down the sensing fibre indicating spatial resolution of ~2m.

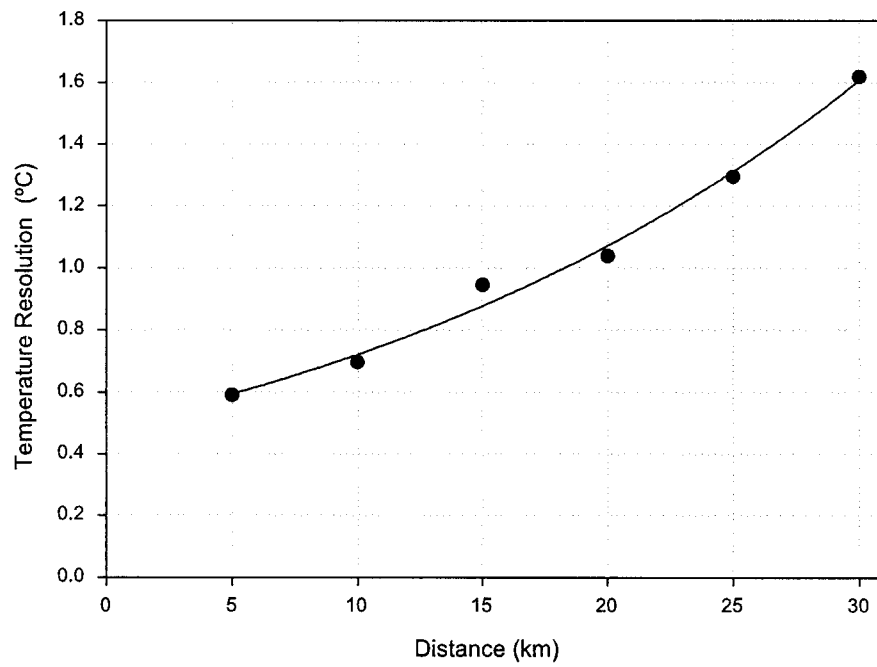
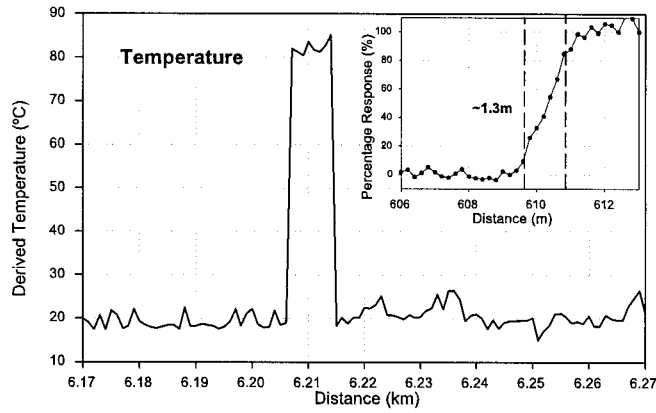
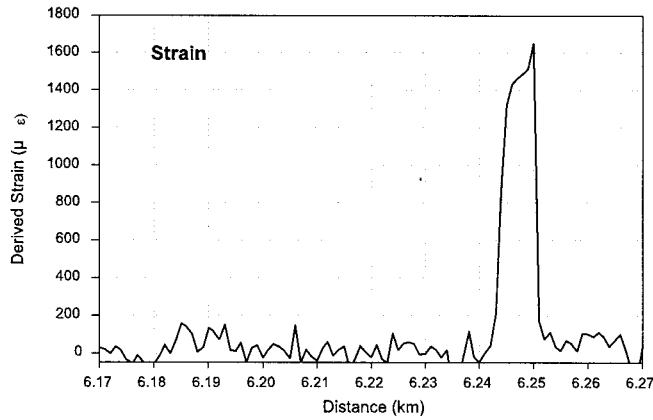


Figure 5. The RMS temperature errors for the 20ns pulse width measurements along the sensing fibre at 5km intervals average over a length of 500m.

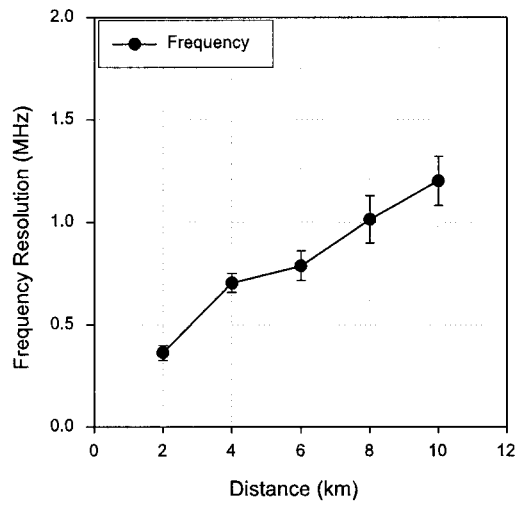


(a) Temperature variation

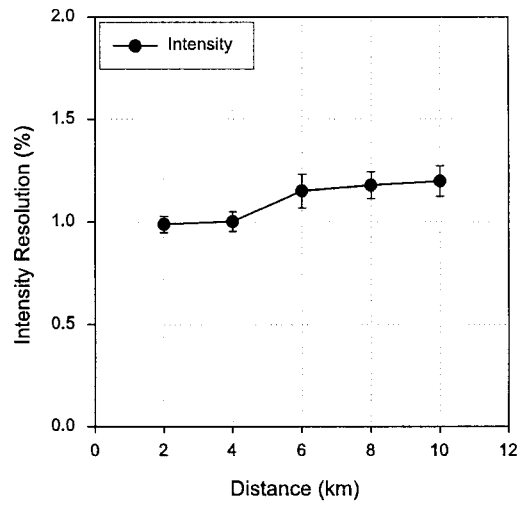


(b) Strain variation

Figure 6. (a)The derived temperature and (b)the derived strain for the simultaneous temperature and strain measurements respectively. The inset graph in (a) verified the $\sim 1.3\text{m}$ spatial resolution measured at 600m down the sensing fibre, which is defined by 10-90% percentage response.



(a) Frequency resolution



(b) Intensity resolution

Figure 7. (a)RMS error in frequency (b)Rms error in intensity taken over 100m window at 2km intervals. The error bars indicate ± 1 Standard Deviation.

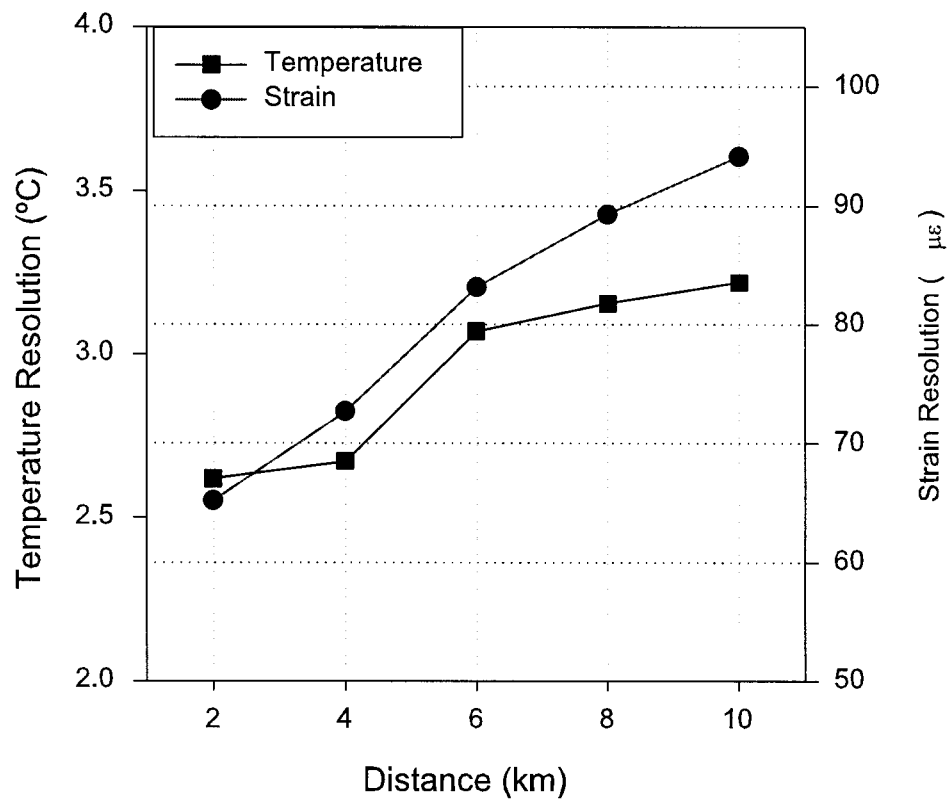


Figure 8. Derived resolutions of temperature (left) and strain (right) based upon the measured data in figure 7.